CHAPTER 2

Hydraulics of Selected Hydraulic Structures

Hubert Chanson[1,*] and *Stefan Felder*[2]

INTRODUCTION

Hydraulic structures are human-made systems interacting with surface runoff in urban and rural environments including structures to assist stormwater drainage, flood mitigation, coastal protection, or enhancing and controlling flows in rivers and other water bodies. The structures may be built across a natural stream to divert, control, store, and manage the water flow: for example, a weir across a waterway and its upstream reservoir controlling both upstream and downstream water levels (Figs. 1 and 2). Hydraulic structures can be designed pro-actively to control the water flow motion: for example, a series of drop structures along a mountain river course built to stabilize the river bed by dissipating the flow energy along the drops. The construction of weirs, dams, and hydraulic structures is possibly the oldest and most important civil engineering activity (Schnitter 1994; Levi 1995). Life on our planet is totally dependent upon water and only two species build hydraulic structures: humans and beavers. The latters are called "*the engineers of Nature*" (Dubois and Provencher 2012). Although the date and location of the most ancient hydraulic structures are unknown, some very famous heritage structure includes the Sumerian irrigation canals in Mesopotamia (BC 3,000), the Sadd-El-Kafara dam in Egypt (BC 2,500), the Marib dam and its irrigation canals in Yemen (BC 750), the Dujianyan irrigation system in China (BC 256), and the Vichansao canal and its diversion structure in the Moche Valley, South America (AD 200).

The two key technical challenges in hydraulic structure design are the conveyance of water and dissipation of kinetic energy. Conveyance implies the transport of water, for example, into the spillway of a dam. The conveyance of the structure is closely linked to the intake design, for example the spillway crest, and chute design (Fig. 3).

[1] The University of Queensland, School of Civil Engineering, Brisbane QLD 4072, Australia.
[2] The University of New South Wales, School of Civil and Environmental Engineering, Sydney NSW 2052, Australia.
E-mail: s.felder@unsw.edu.au
* Corresponding author: h.chanson@uq.edu.au

Its estimate is based upon fundamental fluid dynamic calculations, with a range of proven solutions. Figure 1D illustrates a rounded spillway crest designed to increase the discharge capacity at design flow compared to a broad crest. The dissipation of energy occurs along the chute and at its downstream end. The available energy can be very significant and kinetic energy dissipation must take place safely before the water rejoins the natural river course. With many structures, a major challenge is the magnitude of the rate of energy dissipation at design and non-design flow conditions. The design of the energy dissipators relies upon some sound physical modelling combined with solid prototype experiences (Novak et al. 1996; Vischer and Hager 1998; Chanson 2015).

The rate of energy dissipation at hydraulic structures can be enormous and its design is far from trivial. For example, the Choufu weir (Fig. 1A) discharging 120 m^3/s with a 2 m high drop would dissipate turbulent kinetic energy flux per unit time at a rate of 2.4 MW. Many engineers have never been exposed to the complexity of dissipator designs, to the hydrodynamic processes taking place, and to the structural challenges. Often hydraulic structures are tested for design discharges, but smaller discharges can result in instationary flow transitions leading to more complex flows and increased hydrodynamic forces on the structure. Numerous spillways, energy dissipators, and storm waterways failed because of poor engineering design (Hager 1992; Novak et al. 2001). A known issue has been a lack of understanding of basic turbulent dissipation processes and the intrinsic limitations of physical and numerical models (Novak and Cabelka 1981; Chanson 2015). Physical studies are conducted traditionally using a Froude similitude implying drastically smaller laboratory Reynolds numbers than in the corresponding prototype flows. Despite advances, the extrapolation of laboratory results to large size prototype structures must be carefully checked, including the implications in terms of numerical model validation and numerical data quality.

Hydraulics of Small Dams and Weirs

Presentation

Dams and weirs are built across a stream or river to facilitate water storage (Fig. 1). A weir is a structure designed to raise the upstream water level to increase water storage and irrigation capacity, and to enable navigation. During large floods, the water is allowed to pass over the top of the full length of the weir. There are several types of weirs defined by their weir shape and crest length. A particular type of structure is the minimum energy loss (MEL) weir (McKay 1975; Chanson 2003); a MEL weir is designed to minimize the total head loss of overflow, thus inducing zero afflux for the design flow in the case of the structure shown in Fig. 2A. A dam is defined as a large structure built across a valley to store water in the upstream reservoir for flood mitigation, hydroelectricity, or water supply. The upstream water elevation should not overtop the dam wall, because it would lead indeed to dam erosion and possibly destruction. During large rainfalls, large inflows enter the dam reservoir, and a spillway structure must be designed to spill the flood flow beside, below, through, or above the dams, under controlled conditions (USBR 1987; Novak et al. 2001). Most small dams are equipped with an overflow spillway system (Fig. 3). The overflow spillway consists typically of three sections: the crest, the steep chute, and the stilling structure

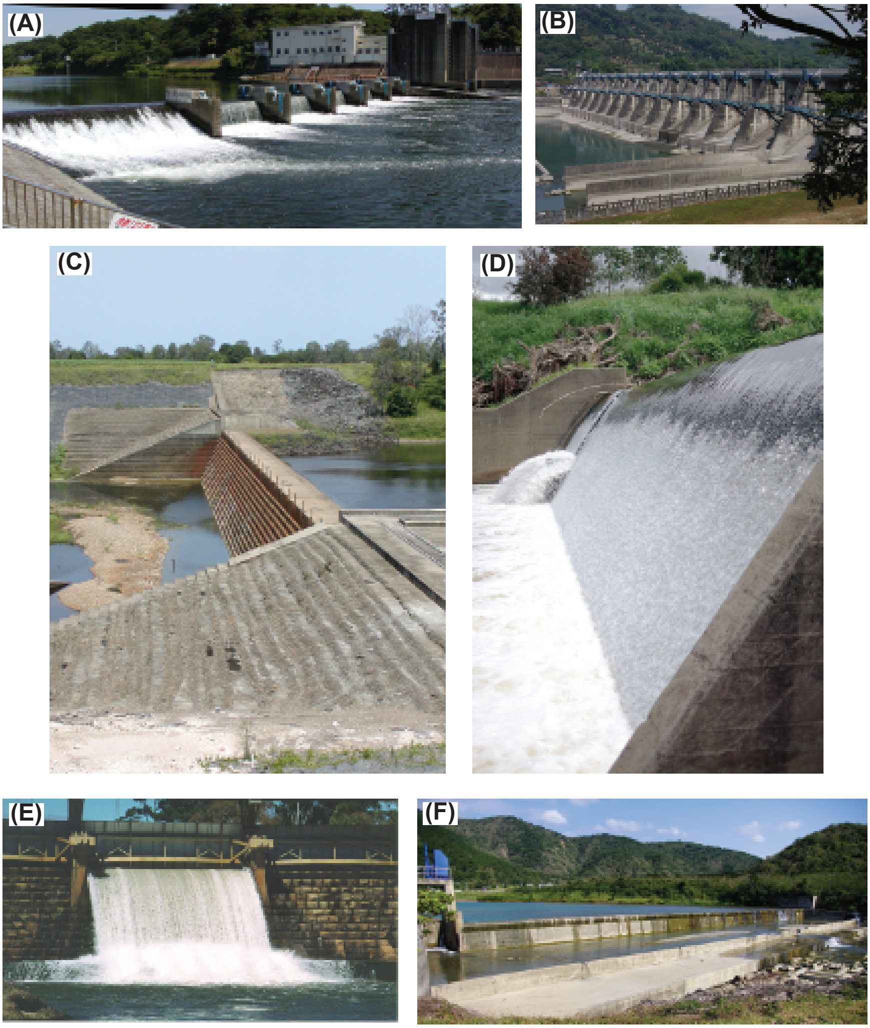

Fig. 1. Photographs of hydraulic structures and weirs along river courses: (A) Choufu weir on Tama River (Japan); (B) Shih Kang Dam (Taichung, Taiwan); (C) Bucca weir (Bundaberg QLD, Australia); (D) Jordan weir (Gatton QLD, Australia); (E) Goulburn weir (VIC, Australia); (F) Chenchung weir (Pingtung, Taiwan).

at the downstream end. The crest and chute are designed to carry safely the flood flow, while the stilling basin is designed to break down the kinetic energy of the flow before reaching the downstream river channel.

During the design stage, the engineers select the optimum spillway shape for the design flow conditions. Then the safe operation of the spillway must be checked for a range of operating flow conditions ($Q<Q_{des}$) and for emergency situations ($Q>Q_{des}$), where Q is the discharge and Q_{des} is the design discharge.

Fig. 2. Unusual weir designs in Australia: (A) Minimum energy loss weir on the Condamine River (Chinchilla, QLD); (B) Timber crib weir on MacIntyre Brook (Whetstone weir, QLD).

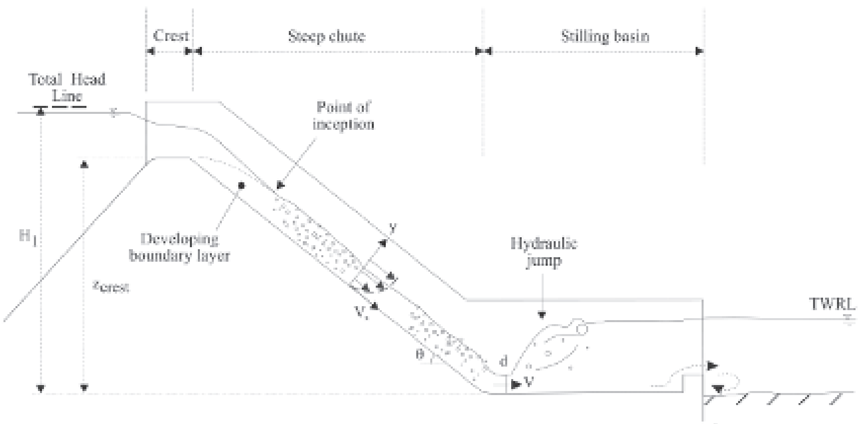

Fig. 3. Cross-sectional sketch of small dam spillway.

Conveyance and Crest Design

For an overflow spillway design, the crest of the spillway is basically designed to maximize the discharge capacity of the structure. In open channels and for a given specific energy, maximum flow rate is achieved for critical flow conditions (Bélanger 1828; Bakhmeteff 1912), and critical flow conditions are observed at the weir crest (Chanson 2006), unless the crest is drowned. For a rectangular spillway crest, the discharge per unit width q may be expressed as:

$$q = C_D \sqrt{g} \left(\frac{2}{3} (H_1 - z_{crest}) \right)^{3/2} \quad \text{with critical flow conditions} \tag{1}$$

where C_D is the dimensionless discharge coefficient, g is the gravity acceleration, H_1 is the upstream total head and z_{crest} is the spillway crest height (Fig. 3).

When the crest is broad enough ($L_{crest}/(H_1–z_{crest})>1.5$ to 3), the streamlines are parallel to the crest invert and the pressure distribution above the crest is hydrostatic (Hager and Schwalt 1994; Felder and Chanson 2012). Despite some scatter, experimental data for broad-crested weir with rounded corner yielded a discharge coefficient C_D of about unity:

$$C_D = 0.934 + 0.143 \frac{H_1 - z_{crest}}{L_{crest}} \quad \text{broad-crested weir for } H_1/L_{crest}>0.1 \tag{2}$$

where L_{crest} is the broad-crest length. Equation (2) is compared with data in Fig. 4A. For $H_1/L_{crest}<0.1$, the flow is near-critical along the crest and some stable undulations of the free-surface are present (Fig. 4A).

Rounded crest designs can achieve a larger discharge for the same head above crest than a broad-crested weir ($C_D>1$). A simple rounded design is the circular crest of radius R. The analysis of experimental data with partially-developed inflow conditions yielded (Chanson and Montes 1998):

$$C_D = 1.13 \left(\frac{H_1 - z_{crest}}{R} \right)^{0.18} \quad \text{circular crested weir } (0.5<(H_1–z_{crest})/R<3.5) \tag{3}$$

An efficient design is the ogee crest, for which the pressures at the face of the crest invert are atmospheric at design flow conditions. The profile is basically the trajectory of the underside of a free-falling jet downstream of a two-dimensional sharp crested weir for the design discharge Q_{des} and upstream head H_{des} (Creager 1917; Montes 1992). Figure 4B illustrates typical ogee crest profiles in dimensionless terms with coordinates $X/(H_{des}–z_{crest})$ and $Y/(H_{des}–z_{crest})$ representing the dimensionless locations in x- and y-directions respectively. For the design flow, the discharge coefficient $(C_D)_{des}$ is primarily a function of the crest shape (USBR 1987; Chanson 2004). For an ogee with vertical upstream wall, Fig. 4B presents typical values of $(C_D)_{des}$ as a function of the relative design head above crest $(H_{des}–z_{crest})/z_{crest}$. When the discharge differs from the design flow, the relative discharge coefficient $C_D/(C_D)_{des}$ becomes a function of the relative upstream total head $(H_1–z_{crest})/(H_{des}–z_{crest})$ (Fig. 4B). For $H_1<H_{des}$, $Q<Q_{des}$ and the pressure on the crest invert is larger than atmospheric. For very low flows (i.e.,

$H_1 << H_{des}$), the discharge coefficient tends to unity: that is, the broad-crested weir case. When $H_1 > H_{des}$, the pressures on the crest are less than atmospheric and the discharge coefficient C_D is larger than the design discharge coefficient $(C_D)_{des}$. Such flow conditions are exceptional and cavitation might occur on the crest profile.

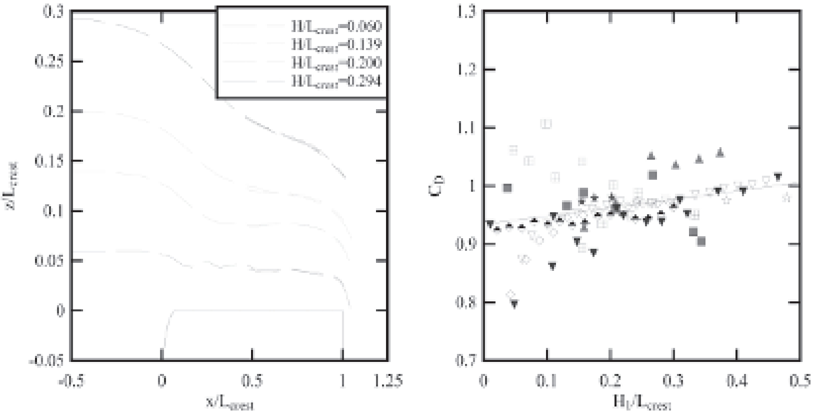

(A) Broad crested weir with upstream rounded corner: dimensionless free-surface profiles (Data: Felder and Chanson 2012) and dimensionless discharge coefficient data (Data: Vierhout 1973; Bazin 1896; Gonzalez and Chanson 2007; Felder and Chanson 2012; Zhang and Chanson 2015; Felder 2015).

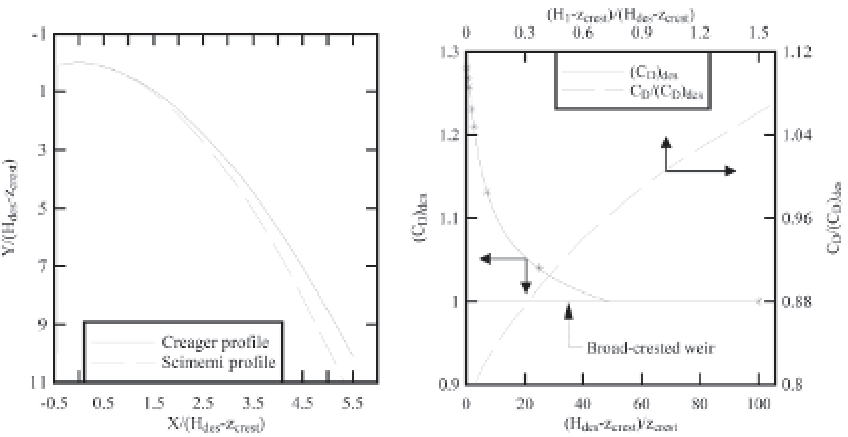

(B) Ogee crest with vertical upstream wall: typical crest profiles and discharge coefficient.

Fig. 4. Spillway crest overflow performances.

Downstream of the crest, the fluid is accelerated by gravity along the steep chute (Fig. 3). A turbulent boundary layer is generated by bottom friction at the upstream end and the boundary layer thickness increases with increasing distance along the chute. When the outer edge of the boundary layer reaches the free-surface, the flow becomes fully-developed and free-surface aeration takes place over a very small distance in rapidly varied flows (Fig. 3). Figures 1D and 7A illustrate the inception point of free-surface aeration, clearly visible with the apparition of white waters. Downstream of the inception point in the fully-developed flow region, the flow is gradually-varied until it reaches equilibrium. The gradually-varied flow properties may be calculated based upon the backwater equation, while the uniform equilibrium flow conditions (normal flow conditions) may be estimated based upon momentum considerations (Henderson 1966; Chanson 2004).

On a steep chute, both the flow acceleration and boundary layer development affect the flow properties. The complete flow calculations can be tedious. Combining physical observations with developing and uniform equilibrium flow calculations, a general trend may be derived for preliminary designs (Bradley and Peterka 1957; Henderson 1966; Chanson 1999, 2004). In absence of losses, the maximum ideal velocity at the chute's downstream chute would be:

$$V_{max} = \sqrt{2g(H_1 - d\cos\theta)} \tag{4}$$

where d is the downstream flow depth ($d = q/V_{max}$), q is the discharge per unit width and θ is the chute slope (Fig. 3). In reality the flow velocity V is smaller than the theoretical velocity V_{max} because of energy losses down the chute. Figure 5 summarizes the dimensionless flow velocity at the end of the steep chute V/V_{max} as a function of the dimensionless upstream head H_1/d_c where d_c is the critical depth ($d_c=(q^2/g)^{1/3}$). Both developing and uniform equilibrium flow calculations are presented for smooth and stepped chutes. Prototype smooth chute data and laboratory stepped chute data are included for comparison using an average Darcy friction factor of f=0.03 for the smooth chutes and of f=0.2 for the stepped chute. The results are valid for smooth and stepped spillways (concrete chutes) with slopes ranging from 18º to 55º.

Comparing stepped and smooth chutes, larger energy dissipation rates are systematically observed along a stepped spillway because of a predominance of form drag compared to friction drag on the smooth invert. Hence the residual energy at the

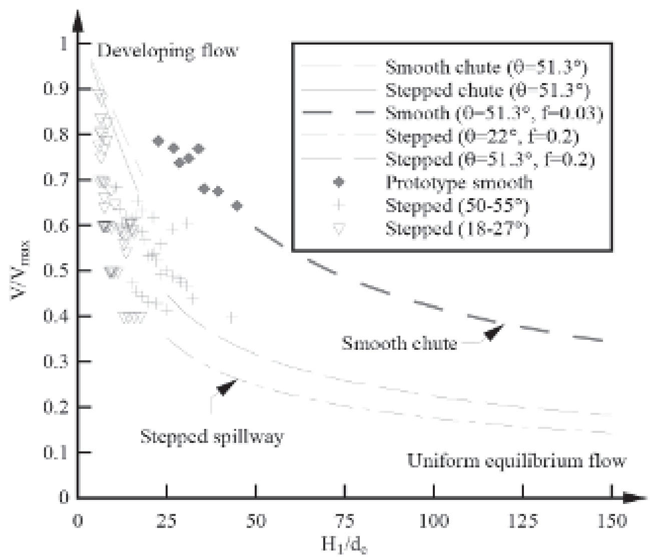

Fig. 5. Velocity at a steep chute toe. Comparison between smooth and stepped invert configurations.

downstream end of a stepped chute will be smaller and the size of the downstream stilling basin can be reduced (e.g., Felder and Chanson 2013). The form drag results in larger mean bottom shear stress, implying larger hydrodynamic loads on the steps than on a smooth invert.

Energy dissipation

At the downstream end of the spillway system, the excess in kinetic energy must be dissipated before the flow re-joins the natural stream. Energy dissipation may be achieved by a hydraulic jump stilling basin downstream of the steep chute, a high velocity water jet taking off from a flip bucket and impinging into a downstream plunge pool, and a plunging jet pool in which the spillway flow impinges and the kinetic energy is dissipated in turbulent recirculation (Figs. 1 and 2) (USBR 1965; Novak et al. 2001; Chanson 2015). The design of a stepped chute may assist also in energy dissipation (Figs. 1C and 2B).

A hydraulic jump stilling basin is the common type of dissipators for small dams and weirs. Most kinetic energy is dissipated in the hydraulic jump, sometimes assisted by appurtenances (step, baffles) to increase the turbulence. A hydraulic jump is the rapid and sudden transition from a supercritical to subcritical flow. The jump is an extremely turbulent process, and the large-scale turbulence region is typically called the roller. The downstream flow depth d_{conj} (conjugate depth) and energy loss DH in the jump may be deduced from the momentum principle. For a flat horizontal rectangular channel:

$$\frac{d_{conj}}{d} = \frac{1}{2}\left(\sqrt{1+8Fr^2}-1\right) \tag{5}$$

$$\frac{\Delta H}{d} = \frac{\left(\sqrt{1+8Fr^2}-3\right)^3}{16\left(\sqrt{1+8Fr^2}-1\right)} \tag{6}$$

where $Fr=V/(gd)^{1/2}$ is the inflow Froude number, and d and V are the inflow depth and velocity (Fig. 3).

Hydraulic jump flows may exhibit different patterns depending upon the upstream Froude number spanning from undular jumps for Froude numbers close to and slightly above unity, to steady and strong jumps for large Froude numbers. In practice, it is recommended to design energy dissipators for $4.5<Fr<9–10$, although some standard stilling basins may be devised for lower inflow Froude number conditions. An important design parameter is the roller length L_r, which may be estimated from experimental observations:

$$\frac{L_r}{d} = 6\,(Fr-1) \tag{7}$$

Equation (7) is valid for rectangular horizontal channels and $2<Fr<10$.

The hydraulic design of the stilling basin must ensure the safe dissipation of the kinetic energy of the flow and minimize the size of the stilling structure. In practice, energy dissipation by the hydraulic jump may be assisted by elements (e.g., baffle blocks, sill) placed on the stilling basin apron (Fig. 6). In all cases, the length of a hydraulic

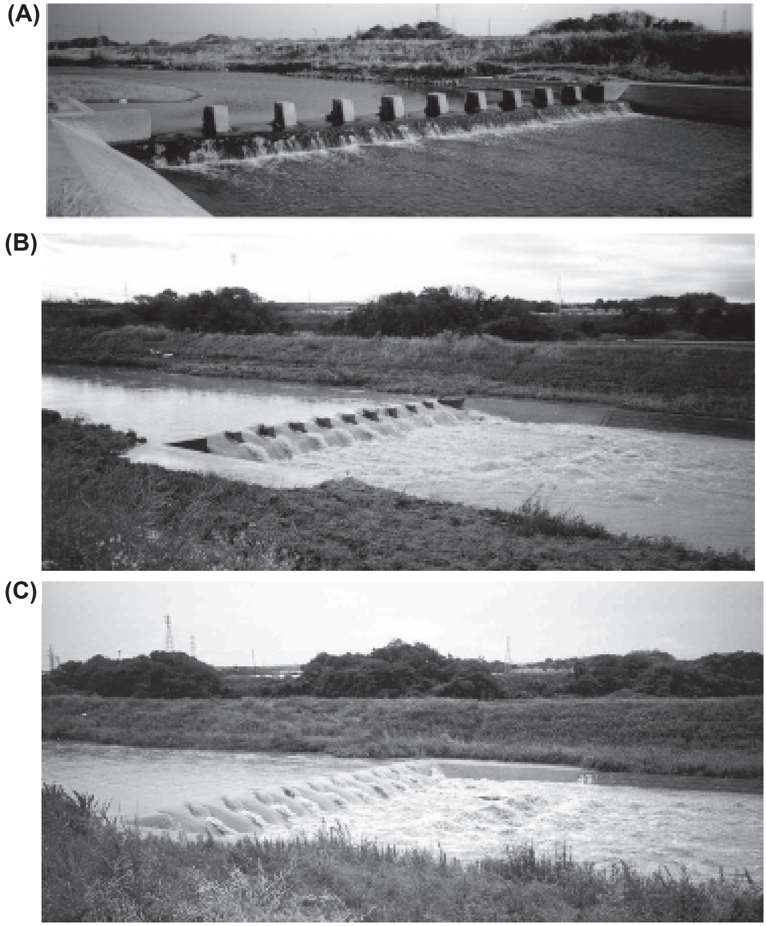

Fig. 6. Operation of a small stilling structure in Toyohashi (Japan) during very-low (Top), low (Middle), and medium flows (Bottom).

jump stilling basin must be greater than the roller length for all flow conditions. Basic aperture of stilling basins may include drop, sill, baffle blocks, sudden expansion (Hager 1992). A number of standard stilling basin designs were developed in the 1940s to 1960s (Chanson and Carvalho 2015). Each basin design was tested in models and prototypes over a considerable range of flow conditions. Their performances are well known, and they can be selected without further model studies within their design specifications. In practice, design engineers must ensure that the energy dissipation takes place in the spillway system and that the stilling basin can operate safely for a wide range of flow conditions. Damage (scouring, abrasion, cavitation) to the basin and to the downstream natural bed may occur for a number of reasons as discussed by USBR (1965), Chanson (1999), and Novak et al. (2001), including insufficient length of and dissipation structures in the basin or the design for an insufficient range of transitional flow rates as well as flows exceeding the design discharge.

Design procedure

The construction of a small dam and weir across a river has impacts on both the upstream and downstream flow conditions. The weir crest elevation must be selected accurately to provide the required water storage and upstream water level rise, while the spillway system must operate safely for a wide range of flow conditions including tailwater levels and non-design flow rates.

For the simple design of an overflow spillway with hydraulic jump energy dissipation at the chutes downstream end (Fig. 3), the design procedure is (USBR 1965; Chanson 1999):

a) Select the spillway crest elevation z_{crest} based upon reservoir bathymetry, topography, and required storage level.
b) Choose the spillway crest width B based upon site geometry and hydrology.
c) Determine the design discharge Q_{des} from risk analysis and flood routing. The peak spillway discharge is deduced from the combined analysis of storage capacity, and inflow and outflow hydrographs. Potential increases in rainfall over the life of the structure should be taken into account.
d) Calculate the upstream head above spillway crest (H_{des}–z_{crest}) for the design flow rate Q_{des}, as a function of crest geometry and the associated discharge coefficients (Eq. (1)).
e) Select the spillway chute type (smooth or stepped).
f) Choose the chute toe elevation. The stilling basin level may differ from the natural bed level (i.e., tailwater bed level).
g) For the design flow conditions, calculate the flow properties d and V at the end of the chute toe, the conjugate depth for the hydraulic jump, and the roller length L_r. Note that the apron length must be greater than the jump length.
h) Compare the jump height rating level (JHRL) to the natural downstream water level (i.e., tailwater rating level TWRL). If the JHRL does not match the TWRL, the apron elevation, spillway width, design discharge, chute type, and crest elevation must be altered, and the process becomes iterative.

The tailwater rating level TWRL is the natural free-surface elevation in the downstream flood plain (Fig. 3). The downstream channel typically operates in a subcritical flow regime controlled by the downstream/tailwater flow conditions. The jump height rating level JHRL is the free-surface elevation downstream of the hydraulic jump stilling structure. For a horizontal apron, the JHRL is deduced simply from the apron elevation and the conjugate depth. If the apron has an end sill or drop, the JHRL is deduced from the Bernoulli equation, assuming that the hydraulic jump takes place upstream of the sill/drop, and that no energy loss takes place at the sill/drop.

During design stages, engineers are required to compute both the JHRL and the TWRL for all flow rates. The location of the hydraulic jump is determined by the conjugate flow conditions. The upstream depth is the supercritical depth at the steep chute toe and the downstream depth is deduced from the tailwater conditions. The upstream and downstream depths must also satisfy the momentum equation, e.g., Eq. (5) for a horizontal stilling basin in absence of baffles. The results must be compared with the variations in tailwater level (TWRL) for the whole range of discharges.

For a hydraulic jump stilling basin, it is extremely important to consider the following points. The stilling basin is designed for the design flow conditions. For discharges larger than the design discharge, it may be acceptable to tolerate some erosion and damage, but the safety of the dam must be ensured. For discharges less than the design discharge, the energy dissipation must be controlled completely, it must occur in the stilling basin, and there must be no maintenance issue. Figures 6 and 7 show prototype weirs in operation for different flow rates, highlighting a range of tailwater effects on the hydraulic jump. In Fig. 7C, the weir became drowned for very large discharges.

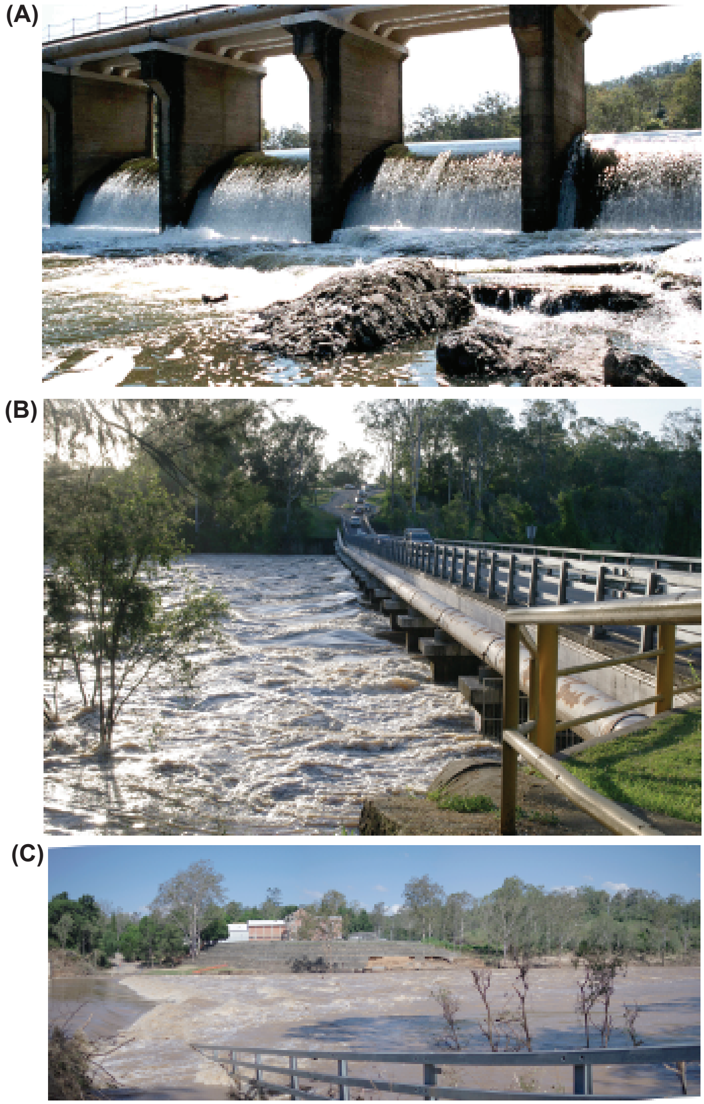

Fig. 7. Operation of Mount Crosby weir on the Brisbane River (QLD, Australia) during low flow (Top), medium flow (Middle), and large flows (Bottom).

Culvert Hydraulics

A culvert is a covered channel designed to pass flood waters, drainage flows, and natural streams through earthfill and rockfill structures (e.g., roadway, railroad). The design can vary from a simple geometry (standard culvert) to a hydraulically-smooth shape (MEL culvert) (Figs. 8 and 9). A culvert consists of three sections: the intake or inlet, the barrel or throat, and the diffuser or outlet. The cross-sectional shape of the barrel may be circular (pipe) or rectangular (box and multi-cell box); a culvert may be designed as a single cell or multiple cell structure.

The hydraulic characteristics of a culvert are the design discharge, the upstream total head and the maximum acceptable head loss from inlet to outlet. The design discharge and upstream flood level are deduced from the hydrological investigation of the site in relation to the purpose of the culvert. Head losses must be minimized to reduce upstream flooding. From a hydraulic engineering perspective, a dominant feature is whether the barrel runs full or not.

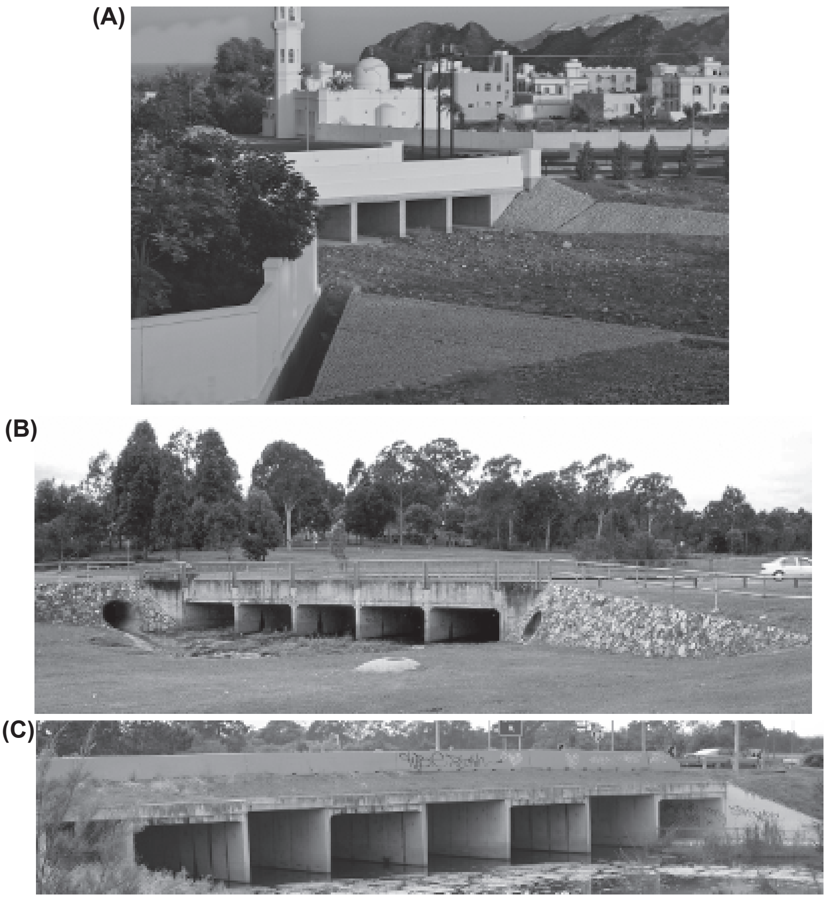

Fig. 8. Box culverts. (A) Muscat, Oman on 31 Oct. 2010 afternoon; (B) Culvert outlet below Ridgewood St, Algester (QLD, Australia) in August 1999; (C) Culvert along Gin House Creek, Carrara, Gold Coast (QLD, Australia) on 5 Dec. 2007.

(A)

(B)

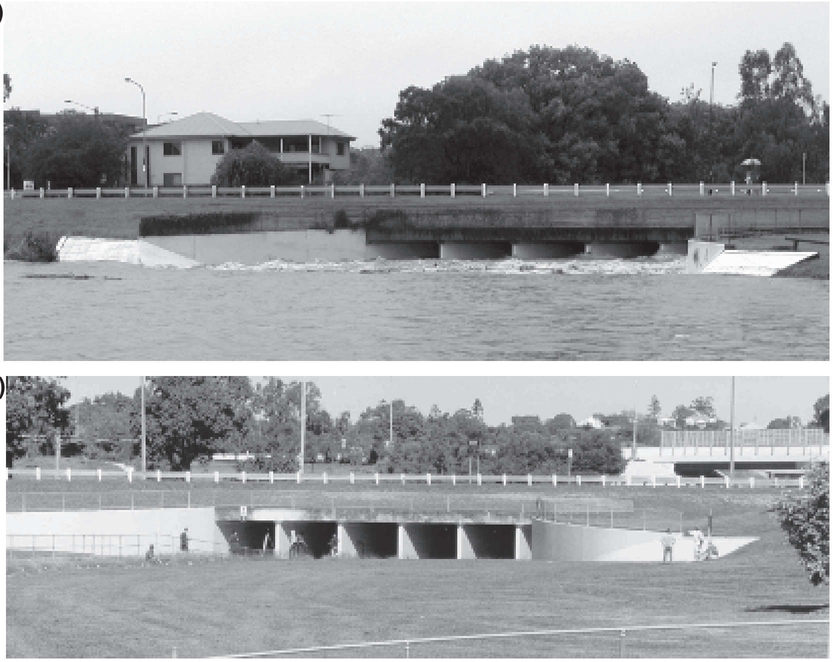

Fig. 9. Minimum energy loss culvert along Norman Creek beneath Ridge Street, Brisbane (Australia). (A) Inlet operation on 7 Nov. 2004 for Q ≈ 80 to 100 m^3/s; (B) Outlet on 13 May 2002.

The hydraulic design of a culvert is basically an optimum compromise between discharge capacity, head loss, and construction costs. While the key objective is to keep the cost of the culvert to a minimum, some consideration must be taken to avoid upstream afflux and flooding by keeping the head loss small and to avoid scour downstream of the culvert outlet if a hydraulic jump might take place by placement of some scour protection. The minimization of head losses and increase in flow performances can be assisted through streamlining of the culvert inlet and outlet including streamlined wings and fans (Figs. 8 and 9). Most culverts are designed to operate as open channel systems, with critical flow conditions occurring in the barrel in order to maximize the discharge per unit width and to reduce the barrel cross-section. Figure 9A shows a typical operation, for a discharge less than the design discharge.

Hydraulics of box culverts

For standard box culverts, the culvert flow may exhibit various flow patterns depending upon the discharge, the upstream head above the inlet invert (H_1–z_{inlet}), the tailwater depth d_{tw}, the bed slope S_o, and the barrel's internal height D (Hee 1969; Chanson 1999). Free-surface inlet flows take place typically for (H_1–z_{inlet})/D<1.2, and submerged inlet operation occurs for (H_1–z_{inlet})/D>1.2. In each case, different flow patterns may occur depending upon the hydraulic control location: that is, inlet control or outlet control (Hee 1969). The transition from free-surface to submerged inlet and the transition from free-surface flows along the barrel to fully drowned flow conditions can be associated with three-dimensional flows at the inlet and along the barrel and instationarities linked to changes from free-surface to pressurized flow conditions. The discharge capacity of the barrel is primarily related to the flow pattern: free-surface inlet flow, submerged entrance, or drowned barrel. When a free-surface flow occurs in the barrel, the discharge is set only by the entry conditions. When the entrance is submerged, the discharge is determined as an orifice flow using experimentally determined discharge coefficients. With fully drowned culverts, the discharge is determined by the culvert's flow resistance. Nomographs are also commonly used to estimate the discharge characteristics (USBR 1987; Concrete Pipe Association of Australasia 1991; Chanson 2004).

For standard culverts, the design procedure can be divided into two parts (Herr and Bossy 1965). First a system analysis must be carried out to ascertain the culvert purposes, design data, constraints. This first stage leads to the estimate of the design flow Q_{des} and the design upstream total head H_{des}. During the second stage, the barrel size is selected by an iterative procedure, in which both inlet control and outlet control calculations are conducted. At the end, the optimum size is the smallest barrel size allowing for inlet control operation. The construction cost may be optimized using a multi-cell culvert of precast circular or rectangular box elements.

Hydraulics of minimum energy loss (MEL) culverts

A minimum energy loss (MEL) culvert is a structure designed with the concept of minimum head loss. In the approach channel, the flow is smoothly contracted through a streamlined inlet into the barrel and then it is expanded in a streamlined outlet before being released into the downstream natural flood plain (Figs. 9 and 10B) (Apelt 1983, 1994; Chanson 1999). The inlet and outlet must both be streamlined to avoid major form losses. The barrel invert is sometimes lowered to increase the discharge capacity since:

$$\frac{Q}{B_{min}} = \sqrt{g}\left(\frac{2}{3}(H_1 - z_{inlet} - \Delta z)\right)^{3/2} \tag{8}$$

where Dz is the barrel invert elevation below the natural ground level (Fig. 10B). The inlet and outlet must both be streamlined to avoid major form losses. The barrel invert is sometimes lowervides less energy loss of the same discharge Q and barrel width B_{min}. An alternative design includes a narrower barrel width for the same discharge and head loss. Successful prototype experiences showed that there are a wide range of design options (McKay 1970, 1978; Cottman and McKay 1990; Chanson 2003, 2007).

The basic design concepts of MEL culverts are: (a) streamlining and (b) critical flow conditions from the inlet lip to the outlet lip at design flow conditions (Apelt 1983). The intake must be designed with a smooth contraction into the barrel and the outlet must be shaped as a smooth expansion back to the natural channel: that is, the flow streamlines must follow very smooth curves and no separation be observed. Minimum energy loss culverts are designed to achieve critical flow conditions in the entire waterway: that is, in the inlet, at the barrel and in the outlet (Fig. 10B).

Professor C.J. Apelt devised a simple design method to estimate the basic characteristics of a MEL culvert (Apelt 1983).

1) Decide the design discharge Q_{des} and the associated total head line (THL) based upon the flow conditions upstream of the culvert.

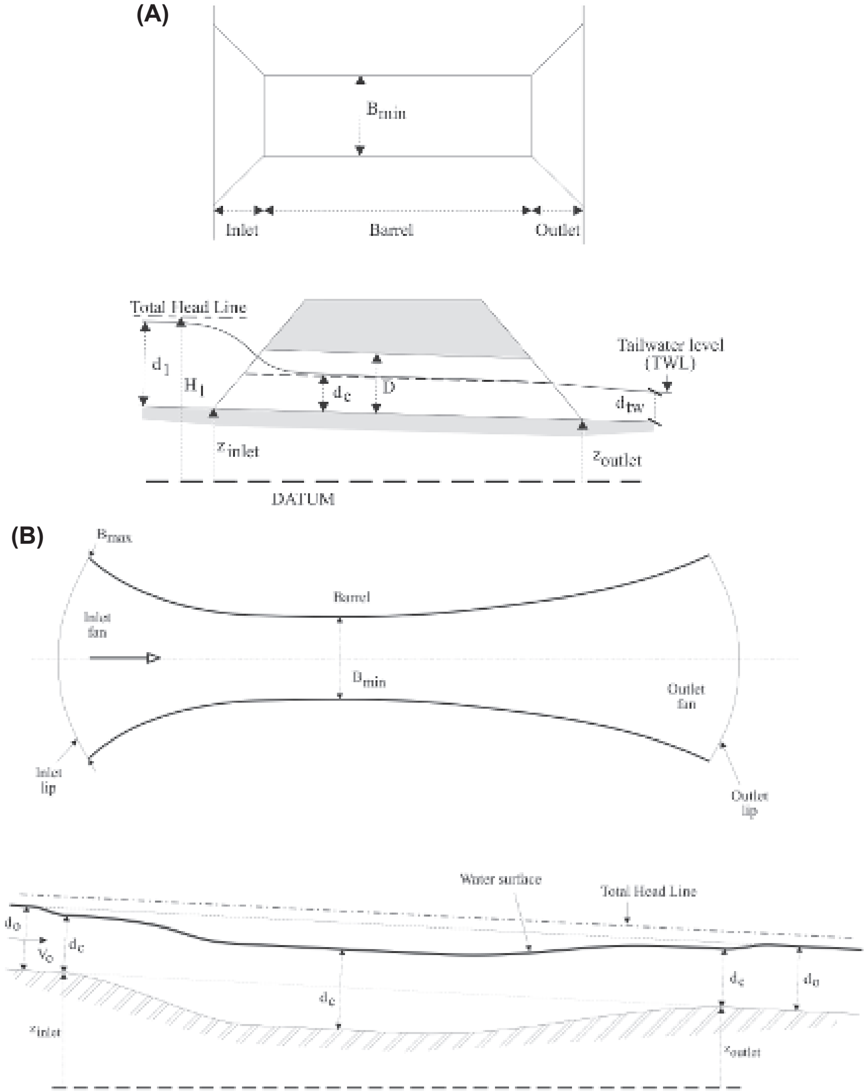

Fig. 10. Definition sketch of culvert hydraulics. (A) Box culvert; (B) Minimum energy loss (MEL) culvert.

2) First neglect energy losses
   2.1) Calculate the waterway characteristics in the barrel for critical flow conditions.
   2.2) Calculate the inlet and outlet lip width B_{max} assuming critical flow conditions and natural bed elevation. The lip width is an equipotential and must be measured along a smooth line normal to the streamlines (Fig. 10B).
3) Decide the shapes of the inlet and outlet.

4) Calculate the geometry of the inlet and outlet to satisfy critical flow conditions everywhere. The contour lines of the inlet and outlet are defined each by their bed elevation to satisfy critical flow conditions, the corresponding width B measured along a smooth line normal to the streamlines, and the longitudinal distance from the lip.
5) Then include the energy losses: namely friction losses along the culvert since the form losses are minimized.
   5.1) Adjust the bed profile of the culvert system to take into account the energy losses. For a long barrel, the barrel slope is selected to be the critical slope.
6) Check the performances of the MEL culvert for non-design conditions for $Q<Q_{des}$ and $Q>Q_{des}$.

The above method gives a preliminary design and full calculations are required later to predict accurately the free-surface profile, complemented by physical modelling (Apelt 1983; Chanson 1999). A correct operation of MEL waterways and culverts requires a proper design. Separation of flow in the inlet and in the outlet must be avoided and head losses must be accurately predicted. Since MEL culverts are designed for critical flow along the entire culvert structure from inlet lip to outlet lip, free-surface undulations may occur, typically in the culvert barrel, and the sidewall of the culvert must be sufficiently high.

Altogether the MEL design technique allows a drastic reduction in the upstream flooding associated with lower costs. The successful operation of MEL culverts for more than 40 years demonstrates the design soundness, while highlighting the importance of the hydraulic expertise of the design engineers (Apelt 1983; Chanson 2007).

Dam Failure and Dam Break Wave

Failures of dams, weirs, and reservoirs during the 19th and 20th centuries led to research into dam break waves. During the second half of the 20th century, two major failures were the Malpasset dam (France) break in 1959 and the overtopping of the Vajont dam (Italy) in 1963 (Fig. 11). Figure 11A shows the remains of the Malpasset dam; on 2 December 1959, the dam collapsed completely and more than 300 people died in the catastrophe.

The propagation of a dam break wave can be predicted analytically for a number of well-defined boundary conditions. For an ideal dam break wave over a dry rectangular channel, the method of characteristics yields an analytical solution first proposed by Ritter (1892):

$$U = 2\sqrt{g\,d_o} \tag{9}$$

$$\frac{x}{t} = 2\sqrt{g\,d_o} - 3\sqrt{g\,d} \tag{10}$$

$$V = \frac{2}{3}\sqrt{g\,d_o}\left(1 + \frac{x}{t\sqrt{g\,d_o}}\right) \tag{11}$$

where U is the dam break wave celerity, d_o is the initial reservoir height, d and V are the water depth and velocity at a location x at time t (Fig. 12).

(A)

(B)

Fig. 11. Dam failures. (A) Malpasset dam, Fréjus, France in September 2004 (Courtesy of Sylvia Briechle); (B) Farm dam failure near Biggenden (QLD, Australia) on 5 March 2013.

The dam break flow with friction may be analyzed as an ideal-fluid flow region led by a friction-dominated tip zone (Fig. 12). Whitham (1955) introduced this conceptual approach, and a complete solution was presented by Chanson (2009). In the tip region ($x_1<x<x_s$), the flow velocity is about the wave front celerity U. When the friction is dominant and the acceleration and inertial terms are small, the shape of the wave front ($x_1<x<x_s$) is given by:

$$d = \sqrt{\frac{f}{4} \frac{U^2}{g} (x_s - x)} \text{ for } x_1<x<x_s \tag{12}$$

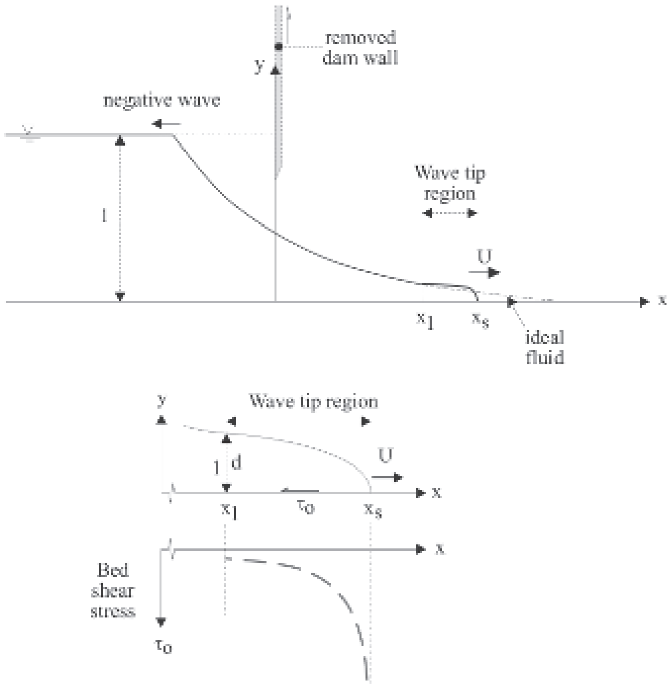

Fig. 12. Definition sketch of a dam break wave and details of the wave tip region.

where the Darcy-Weisbach friction factor f is assumed constant. For $x<x_1$, the free-surface profile follows Eq. (10). At the location $x=x_1$, the transition between ideal fluid and tip regions, the depth and velocity (d_1, V_1) must be continuous and satisfy:

$$d_1 = \frac{d_o}{9}\left(2 - \frac{x_1}{t\sqrt{g\,d_o}}\right)^2 = \sqrt{\frac{f}{4}\,\frac{U^2}{g}\,(x_s - x_1)} \tag{13}$$

$$V_1 = U = \frac{2}{3}\left(\sqrt{g\,d_o} + \frac{x_1}{t}\right) \tag{14}$$

Further the conservation of mass yields an exact solution in terms of the wave front celerity

$$t = \frac{8}{3\,f}\,\frac{\left(1 - \frac{U}{2\sqrt{g\,d_o}}\right)^3}{\frac{U^2}{\sqrt{g\,d_o^{\,3}}}} \tag{15}$$

The wave front location equals

$$x_s = \left(\frac{3}{2}\,\frac{U}{\sqrt{g\,d_o}} - 1\right) t\sqrt{g\,d_o} + \frac{4\,g\,d_o^{\,2}}{f\,U^2}\left(1 - \frac{U}{2\sqrt{g\,d_o}}\right)^4 \tag{16}$$

Equation (15) gives the wave front celerity U at a time t. Equation (16) expresses the wave front location x_s as a function of the wave front celerity U. Equations (10) and (12) give the entire free-surface profile.

The theoretical solution is based upon a few key assumptions. Comparisons between the present solutions and experimental results were successful for a fairly wide range of experimental conditions obtained independently; such comparisons constitute a solid validation of the proposed theory (Chanson 2009). It is acknowledged that the present solution is limited to semi-infinite reservoir, rectangular channel, and quasi-instantaneous dam break. The latter approximation is often reasonable for concrete dam failure (Fig. 11A) but it is not applicable to many other applications, including an embankment breach (Fig. 11B).

Conclusion

For millennia, hydraulic structures have enabled the establishment of human settlements and the development of societies. Man-made hydraulic structures play an important role in mitigating, controlling, storing, and diverting waters in water supply, irrigation, drainage, and stormwater systems, as well as in and along rivers, natural streams, and artificial channels. The design of hydraulic structures must be based upon a sound knowledge of the hydrological and topographical conditions of the catchment to provide design flow estimates and upon advanced engineering expertise in the hydrodynamics of flow processes upstream, downstream, and along the hydraulic structure. For a range of flow rates smaller than or equal to the design flow rate, the structure must allow for conveyance and energy dissipation performances without any damage to the structure and its surroundings. For flow rates in excess of the design flow rate, the structural integrity must be guaranteed.

This chapter provides a brief overview of the engineering design of several hydraulic structures including weirs, small dams, and culverts. For a typical small dam, a key challenge is the design of a structure capable to pass a range of flow conditions without compromising the safety of the structure and the surrounding environment. A similar approach is essential for the design of culvert structures, including box and MEL culverts. Key considerations further encompass the safe passage of flood waters through embankments and associated energy dissipation, as well as a small afflux and minimum costs. Sound engineering design is typically accompanied by thorough physical modelling and engineering design expertise. Despite some advance in numerical modelling, a sound approach relies upon the expert knowledge and solid understanding of the flow physics by the design engineers.

The last section deals with an extreme scenario: the dam break. A simple analytical solution for an instantaneous dam break wave is derived from the method of characteristics. The method provides a simple explicit solution to the dam break wave problem that is easily understood by students, researchers, and professionals, and may be used in real-time by emergency services to estimate the dam break wave with bed friction.

Finally the design of hydraulic structures relies upon high level technical expertise and first-hand experience in hydrodynamics and hydraulic engineering, particularly in terms of conveyance and energy dissipation. The operational challenges are also numerous and they require a broad and solid technical experience and expertise. Such technical challenges are not always well understood and are often understated.

Acknowledgements

This research is supported by the Australian Research Council (Grants DP0878922 & DP120100481).

Keywords: Hydraulic engineering, weirs, small dams, culverts, dam break wave, conveyance, energy dissipation, minimum energy loss, hydraulic structures.

References

Apelt, C.J. 1983. Hydraulics of minimum energy culverts and bridge waterways. Australian Civil Engineering Transactions, I.E. Aust., Vol. CE25(2): 89–95.

Apelt, C.J. 1994. The Minimum Energy Loss Culvert. Videocassette VHS colour, Dept. of Civil Eng., University of Queensland, Australia, 18 minutes.

Bakhmeteff, B.A. 1912. O Neravnomernom Dwijenii Jidkosti v Otkrytom Rusle. (Varied Flow in Open Channel.) St Petersburg, Russia, 232 pages (in Russian).

Bazin, H. 1896. Expériences Nouvelles sur l'Ecoulement par Déversoir. (Recent Experiments on the Flow of Water over Weirs.) Mémoires et Documents, Annales des Ponts et Chaussées (Paris, France) Sér. 7, 12, 2nd Sem., pp. 645–731 (in French).

Bélanger, J.B. 1828. Essai sur la Solution Numérique de quelques Problèmes Relatifs au Mouvement Permanent des Eaux Courantes. (Essay on the Numerical Solution of Some Problems relative to Steady Flow of Water.) Carilian-Goeury, Paris, France, 38 pages & 5 tables (in French).

Bradley, J.N. and Peterka, A.J. 1957. Hydraulic design of stilling basins: short stilling basin for canal structures, small outlet works and small spillways (Basin III). Journal of Hydraulic Division, Proceedings ASCE, Vol. 83, No. HY05, Paper 1403, 22 pages.

Chanson, H. and Montes, J.S. 1998. Overflow characteristics of circular weirs: effect of inflow conditions. Journal of Irrigation and Drainage Engineering, ASCE 124(3): 152–162.

Chanson, H. 1999. The Hydraulics of Open Channel Flow: An Introduction. Butterworth-Heinemann, 1st edition, London, UK, 512 pp.

Chanson, H. 2000. Introducing originality and innovation in engineering teaching: the hydraulic design of culverts. European Journal of Engineering Education 25(4): 377–391.

Chanson, H. 2003. Minimum Energy Loss Structures in Australia: Historical Development and Experience. Proceedings of 12th National Engineering Heritage Conference, I.E. Aust., Toowoomba Qld, Australia, N. Sheridan Editor, pp. 22–28.

Chanson, H. 2004. The Hydraulics of Open Channel Flow: An Introduction. Butterworth-Heinemann, 2nd edition, Oxford, UK, 630 pp.

Chanson, H. 2007. Hydraulic performances of minimum energy loss culverts in Australia. Journal of Performances of Constructed Facilities, ASCE 21(4): 264–272 (doi:10.1061/(ASCE)0887–3828(2007)21: 4(264)).

Chanson, H. 2009. Application of the method of characteristics to the dam break wave problem. Journal of Hydraulic Research, IAHR 47(1): 41–49 (doi:10.3826/jhr.2009.2865).

Chanson, H. 2015. Energy Dissipation in Hydraulic Structures. IAHR Monograph, CRC Press, Taylor & Francis Group, Leiden, The Netherlands, 168 pp.

Chanson, H. and Carvalho, R. 2015. Hydraulic jumps and stilling basins. pp. 65–104. *In*: Chanson, H. (ed.). Energy Dissipation in Hydraulic Structures. IAHR Monograph, CRC Press, Taylor & Francis Group, Leiden, The Netherlands.

Concrete Pipe Association of Australasia. 1991. Hydraulics of Precast Concrete Conduits. Jenkin Buxton Printers, Australia, 3rd edition, 72 pp.

Cottman, N.H. and McKay, G.R. 1990. Bridges and Culverts Reduced in Size and Cost by Use of Critical Flow Conditions. Proceedings of the Institution of Civil Engineers, London, Part 1, 88: 421–437. Discussion: 1992, 90: 643–645.

Creager, W.P. 1917. Engineering of Masonry Dams. John Wiley & Sons, New York, USA.

Dubois, J.M.M. and Provencher, L. 2012. Beaver dams and ponds. pp. 110–113. *In*: Bengtsson, L., Herschy, R.W. and Fairbridge, R.W. (eds.). Encyclopedia of Lakes and Reservoirs. Springer, Encyclopedia of Earth Sciences Series.

Felder, S. and Chanson, H. 2012. Free-surface profiles, velocity and pressure distributions on a broad-crested weir: a physical study. Journal of Irrigation and Drainage Engineering, ASCE 138(12): 1068–1074 (doi:10.1061/(ASCE)IR.1943-4774.0000515).
Felder, S. and Chanson, H. 2013. Aeration, flow instabilities, and residual energy on pooled stepped spillways of embankment dams. Journal of Irrigation and Drainage Engineering 139(10): 880–887, http://dx.doi.org/10.1061/(ASCE)IR.1943-4774.0000627.
Felder, S. 2015. Pressure, velocity and boundary layer distributions on an embankment weir. Proc. 36th IAHR World Congress, The Hague, The Netherlands, 11 pp.
Gonzalez, C.A. and Chanson, H. 2007. Experimental measurements of velocity and pressure distribution on a large broad-crested weir. Flow Measurement and Instrumentation 18(3-4): 107–113 (doi:10.1016/j.flowmeasinst.2007.05.005).
Hager, W.H. 1992. Energy Dissipators and Hydraulic Jump. Kluwer Academic Publ., Water Science and Technology Library, Vol. 8, Dordrecht, The Netherlands, 288 pp.
Hager, W.H. and Schwalt, M. 1994. Broad-crested weir. Journal of Irrigation and Drainage Engineering, ASCE 120(1): 13–26. Discussion. 12(2): 222–226.
Hee, M. 1969. Hydraulics of culvert design including constant energy concept. Proc. 20th Conf. of Local Authority Engineers, Dept. of Local Govt, Queensland, Australia, paper 9, pp. 1–27.
Henderson, F.M. 1966. Open Channel Flow. MacMillan Company, New York, USA.
Herr, L.A. and Bossy, H.G. 1965. Capacity Charts for the Hydraulic Design of Highway Culverts. Hydraulic Engineering Circular, US Dept. of Transportation, Federal Highway Admin., HEC No. 10, March.
Levi, E. 1995. The Science of Water. The Foundation of Modern Hydraulics. ASCE Press, New York, USA, 649 pp.
McKay, G.R. 1970. Pavement drainage. Proc. 5th Aust. Road Res. Board Conf., Vol. 5, Part 4, pp. 305–326.
McKay, G.R. 1975. Appraisal of constant energy structures. Queensland Division Technical Papers, IEAust. 16(6): 2–15.
McKay, G.R. 1978. Design principles of Minimum Energy Waterways. pp. 1–39. *In*: Porter, K.F. (ed.). Proc. Workshop on Minimum Energy Design of Culvert and Bridge Waterways, Australian Road Research Board, Melbourne, Australia, Session 1.
Montes, J.S. 1992. Curvature Analysis of Spillway Profiles. Proc. 11th Australasian Fluid Mechanics Conference AFMC, Vol. 2, Paper 7E-7, Hobart, Australia, pp. 941–944.
Novak, P. and Cabelka, J. 1981. Models in Hydraulic Engineering. Physical Principles and Design Applications. Pitman Publ., London, UK.
Novak, P., Moffat, A.I.B., Nalluri, C. and Narayanan, R. 1996. Hydraulic Structures. E & FN Spon, London, UK, 2nd edition, 599 pp.
Novak, P., Moffat, A.I.B., Nalluri, C. and Narayanan, R. 2001. Hydraulic Structures. Spon Press, London, UK, 3rd edition, 666 pp.
Ritter, A. 1892. Die Fortpflanzung von Wasserwellen. Zeitschrift Verein Deutscher Ingenieure, Vol. 36, No. 2, 33, 13 Aug., 947–954 (in German).
Schnitter, N.J. 1994. A History of Dams: The Useful Pyramids. Balkema Publ., Rotterdam, The Netherlands.
USBR. 1965. Design of Small Dams. Bureau of Reclamation, US Department of the Interior, Denver CO, USA, 1st edition, 3rd printing.
USBR. 1987. Design of Small Dams. Bureau of Reclamation, US Department of the Interior, Denver CO, USA, 3rd edition.
Vierhout, M.M. 1973. On the boundary layer development in rounded broad-crested weirs with a rectangular control section. Report No. 3, Laboratory of Hydraulics and Catchment Hydrology, Agricultural University, Wageningen, The Netherlands, 74 pages.
Vischer, D. and Hager, W.H. 1998. Dam Hydraulics. John Wiley, Chichester, UK, 316 pp.
Whitham, G.B. 1955. The effects of hydraulic resistance in the dam-break problem. Proceedings of Royal Society of London, Series A 227: 399–407.
Zhang, G. and Chanson, H. 2015. Hydraulics of the developing flow region of stepped cascades: an experimental investigation. Hydraulic Model Report No. CH97/15, School of Civil Engineering, The University of Queensland, Brisbane, Australia, 76 pp.

Bibliography

Chanson, H. 2015. Introduction: energy dissipators in hydraulic structures. pp. 1–9. *In*: Chanson, H. (ed.). Energy Dissipation in Hydraulic Structures. IAHR Monograph, CRC Press, Taylor & Francis Group, Leiden, The Netherlands.

Chanson, H. 2015. Energy dissipation: concluding remarks. pp. 159–165. *In*: Chanson, H. (ed.). Energy Dissipation in Hydraulic Structures. IAHR Monograph, CRC Press, Taylor & Francis Group, Leiden, The Netherlands.

Chanson, H., Bung, D. and Matos, J. 2015. Stepped spillways and cascades. pp. 45–64. *In*: Chanson, H. (ed.). Energy Dissipation in Hydraulic Structures, IAHR Monograph, CRC Press, Taylor & Francis Group, Leiden, The Netherlands.

Dressler, R.F. 1952. Hydraulic resistance effect upon the dam break functions. Journal of Research of the National Bureau of Standards 49(3): 217–225.

Dressler, R. 1954. Comparison of theories and experiments for the hydraulic dam-break wave. Proc. International Association Scientific Hydrology Assemblée Générale, Rome, Italy 3(38): 319–328.

Hee, M. 1978. Selected Case Histories. Proc. Workshop on Minimum Energy Design of Culvert and Bridge Waterways, Australian Road Research Board, Melbourne, Australia, Session 4, Paper 1, pp. 1–11.

McKay, G.R. 1971. Design of minimum energy culverts. Research Report, Dept. of Civil Eng., Univ. of Queensland, Brisbane, Australia, 29 pages & 7 plates.

Montes, J.S. 1992. A Potential Flow Solution for the Free Overfall. Proceedings of Institution of Civil Engineers Water Maritime & Energy, Vol. 96, Dec., pp. 259–266. Discussion: 1995, Vol. 112, Mar., pp. 81–87.

Montes, J.S. 1998. Hydraulics of Open Channel Flow. ASCE Press, New-York, USA, 697 pp.

Tullis, B.P. 2013. Current and future hydraulic structure research and training needs. pp. 3–9. *In*: Bung, D. and Pagliara, S. (eds.). Proceedings of International Workshop on Hydraulic Design of Low-Head Structures, IAHR, 20–22 Feb., Aachen, Germany, Bundesanstalt für Wasserbau, Germany.